Determination of the temperature and time dependence of the absolute small-angle X-ray scattering intensity of partially crystalline polymers employing synchrotron radiation*

R. Gehrke†, C. Riekel‡ and H. G. Zachmann§
Institut für Technische und Makromolekulare Chemie der Universität Hamburg, Bundesstrasse 45, D-2000 Hamburg 13, FRG
(Received 21 November 1988; accepted 24 January 1989)

A method was developed to correct the influence of variations of the cross section of the synchrotron radiation beam on the intensity of small-angle X-ray scattering (SAXS). By means of this method the change of the SAXS intensity of poly(ethylene terephthalate) during heating and cooling was quantitatively evaluated. Three different effects could be distinguished: (1) changes in $\Delta\rho$, the difference between the densities of the crystalline and the amorphous regions, (2) partial melting and (3) recrystallization. By separation of the three effects, it becomes possible to measure the kinetics of partial melting and recrystallization. By comparing the change of the SAXS power Q with the change of the degree of crystallinity as determined by wide-angle X-ray scattering, it was proved that partial melting and recrystallization takes place within the spherulites without changing the spherulitically crystallized volume of the sample. The measurements of $\Delta\rho$ indicate that an orientation of the chains by drawing leads to an increase of the glass transition temperature and to a decrease of the thermal expansion coefficient of the amorphous regions.

(Keywords: synchrotron radiation; small-angle X-ray scattering; melting; recrystallization; poly(ethylene terephthalate))

INTRODUCTION

Small-angle X-ray scattering (SAXS) is an excellent tool for investigation of the changes in the morphology of partially crystalline polymers during crystallization, recrystallization and melting. However, in order to perform real-time measurements of the changes of SAXS while the morphological changes take place, because of the weak scattering of polymers it is necessary to use synchrotron radiation as a very strong source of X-rays in addition to fast position-sensitive detectors. Such measurements as well as the corresponding experimental techniques have been reported in previous publications[1–5] and review articles[6,7].

If the scattering intensities are evaluated quantitatively, problems arise which are due to instabilities of the intensity of the primary beam. Normally, an ionization chamber is placed in the primary beam in order to monitor changes in the intensity of the beam caused by the decrease of the particle current within the storage ring. However, sometimes additional intensity variations occur which cannot be corrected by means of the data obtained via the ionization chamber. Changes in the beam position and in the cross section of the beam seem to be the origin of these variations. They alter the power of that part of the beam which falls on the sample while the total power of the beam stays constant.

In the present publication a method is described to measure the total power of the part of the primary beam which falls upon the sample and gives rise to scattering. By this method the scattering intensity can be evaluated quantitatively, even when changes in the position and in the cross section of the beam occur. The method is used to perform time-resolved measurements of the change of SAXS of poly(ethylene terephthalate) (PET) during heating and cooling.

A change of the SAXS intensity upon heating is caused by the different thermal expansion coefficients of the crystalline and amorphous regions. If partial melting and recrystallization occur, they give rise to additional intensity changes.

The influence of thermal expansion on the scattering power of semicrystalline polymers has previously been discussed by Fischer *et al.*[8]. These authors have shown that, by SAXS measurements, the difference between the linear thermal expansion coefficients of crystalline and non-crystalline regions as well as the glass transition temperature of the non-crystalline phase can be determined. In this paper we apply that method to oriented and unoriented PET.

Partial melting and recrystallization in PET were first studied by Zachmann and Stuart[9,10] by using quenched samples in which different states attained during the corresponding processes were frozen in. In the present paper, time-resolved measurements are performed at the temperature of melting and recrystallization, and new insights into the process of partial melting and recrystallization are obtained by comparing the SAXS results with density measurements.

---

* Dedicated to Professor Doctor E. W. Fischer on the occasion of his 60th birthday

† Present address: HASYLAB at DESY, Hamburg, FRG
‡ Present address: ESRF, Grenoble, France
§ To whom correspondence should be addressed

0032-3861/89/091582-09$03.00

THEORETICAL BACKGROUND

The SAXS intensity integrated over all scattering angles is denoted as the scattering power Q. The scattering power of a partially crystalline polymer forming a two-phase system is given by:

$$Q = cV_s x_{cs}(1 - x_{cs})(\Delta\rho)^2 \quad (1)$$

where V_s is the volume fraction of spherulites or other entities contributing to the SAXS (like packed lamellae, fibrils, etc.), x_{cs} is the degree of crystallinity within those entities and $\Delta\rho$ is the density difference between the crystalline and non-crystalline regions. The primary beam intensity and geometrical factors of the instrument are taken into account by the constant c.

During isothermal crystallization and melting, V_s and/or x_{cs} are changing, resulting in a change of Q. The overall degree of crystallinity, x_c, as measured by density or wide-angle X-ray scattering, is given by:

$$x_c = V_s x_{cs} \quad (2)$$

In the case of isothermal crystallization starting from the molten state, V_s increases from 0 to 1 while x_{cs} is constant or slightly increasing. After the sample volume is totally occupied by spherulites, V_s is 1. The main crystallization, then, is complete. Any further increase in x_c has to be attributed to a corresponding change in x_{cs} (secondary crystallization). In the case of partial melting and recrystallization, it has not been investigated up to now which of the two quantities, V_s or x_{cs}, is changing. An answer to this question is found in the present investigation.

When the temperature is varied, $\Delta\rho$ is changed due to the different thermal expansions of the crystalline and amorphous regions. This, in addition, influences the value of Q. The function giving Q as a function of the temperature T for constant values of x_c and x_{cs} will be denoted by $Q(T)$. In agreement with a previous publication[8], we define the thermal expansion coefficient α as the change of density per degree (°C), i.e. $\alpha = d\rho/dT$, in contrast to the usual definition in thermodynamics, $\alpha = (1/v)dv/dT$. Then, by means of (1), it can easily be shown that, if V_s and x_{cs} stay constant, the following relation holds for $Q(T)$:

$$\left(\frac{Q(T)}{Q(T_0)}\right)^{1/2} = 1 + \frac{\alpha_a - \alpha_c}{\Delta\rho(T_0)}(T - T_0) \quad (3)$$

In this relation it is assumed that the thermal expansion of the crystalline and amorphous phases can be fully described by their linear thermal expansion coefficients α_a and α_c, respectively; T_0 is any reference temperature. If x_{cs} and V_s vary, equation (3) has to be replaced by:

$$\left(\frac{Q(T)V_s(T_0)x_s(T_0)[1 - x_s(T_0)]}{Q(T_0)V_s(T)x_s(T)[1 - x_s(T)]}\right)^{1/2} = 1 + \frac{\alpha_a - \alpha_c}{\Delta\rho(T_0)}(T - T_0) \quad (4)$$

The left-hand side of the equation will be designated by $K_{T_0}(T)$.

EXPERIMENTAL

Preparation of the samples

The investigations were performed on poly(ethylene terephthalate) (PET) synthesized in our laboratory from terephthalic acid dimethyl ester and diethylene glycol by transesterification followed by polycondensation[11]. Antimony trioxide and manganese acetate were used as catalysts. The weight-average molar mass M_w was determined by viscometry in a mixture of phenol and 1,1,2,2-tetrachloroethane using the relationship[12] $[\eta] = 4.68 \times 10^{-4} M_w^{0.68}\ \mathrm{dl\,g^{-1}}$. The M_w of the samples investigated here was 33 000. Films 100 μm thick have been prepared by melt pressing the material under vacuum. The films were then quenched in iced water to yield amorphous samples. Part of the samples were drawn at room temperature on an Instron tensile testing machine. These samples became highly oriented by necking. The birefringence after stretching was about 0.19.

Finally the samples were crystallized in an evacuated glass tube, the ends of the oriented films being fixed.

Density measurements

The densities of the samples were measured by means of a density gradient column consisting of a mixture of n-hexane and carbon tetrachloride. The crystallinities were calculated by assuming a value of $1.334\ \mathrm{g\,cm^{-3}}$ for the density of the amorphous regions and a value of $1.490\ \mathrm{g\,cm^{-3}}$ for the crystal density[13].

Small-angle X-ray scattering

The measurements were performed by means of a double-focusing camera which has been developed by Hendrix, Koch and Bordas[14] at the EMBL outstation at DESY/Hamburg. A wavelength of 0.15 nm obtained by Bragg reflection at the 111-net planes of a germanium single crystal was used. A more detailed description of the camera can be found elsewhere[6].

In order to perform measurements at different temperatures, a furnace has been constructed using a special device which allows the sample to be shot quickly into the preheated furnace (see *Figure 1*). In this furnace, well defined heating and cooling rates of up to $150\ ^\circ\mathrm{C\,min^{-1}}$ can be applied to the sample, and the temperature can also be kept constant with variations of less than $\pm 0.3\ ^\circ\mathrm{C}$. The furnace is mounted in an evacuated tube (see *Figure 2*) in order to keep the sample *in vacuo* all the time during the measurement. The evacuated tube also contains the beam stop. It is closed at its two ends by a mica window and a capton window respectively. An ionization chamber is placed into the beam in front of the mica window outside of the tube. The detector, a one-dimensional position-sensitive Gabriel counter[15], is also placed outside of the tube as close as possible to the capton window.

During the scattering measurements, the power of the primary beam falling upon the sample might fluctuate for various reasons. First, the particle current within the storage ring decreases gradually during the time between injection and the end of the machine cycle. This decrease is detected by the ionization chamber. Secondly, owing to instabilities of the optical elements of the beam line, the primary beam might change its cross section as well as its vertical or horizontal position. Such changes alter the radiation power falling upon the sample and, in the case of widely opened aperture slits which are often necessary in order to obtain high photon flux, they cannot be measured by the ionization chamber. The best way to observe these changes is to measure the primary beam intensity directly behind the sample. For this purpose a

semitransparent beam stop has been constructed, consisting of a lead block with a hole in the middle. The hole is filled with aluminium of appropriate thickness in order to reduce the transmitted intensity to about 10^3 photons/second. This intensity can be directly registered by the Gabriel counter detecting the scattered radiation.

After normalization of the scattering intensities with respect to the primary beam intensity measured behind the sample, the background scattering was subtracted. To obtain the scattering power Q, the data were integrated over all values of $s=(2/\lambda)\sin\theta$ ranging from $s=0$ to $s=0.15\,\mathrm{nm}^{-1}$. With films of 100 μm thickness, the data acquisition time for one single scattering pattern was approximately 20 s.

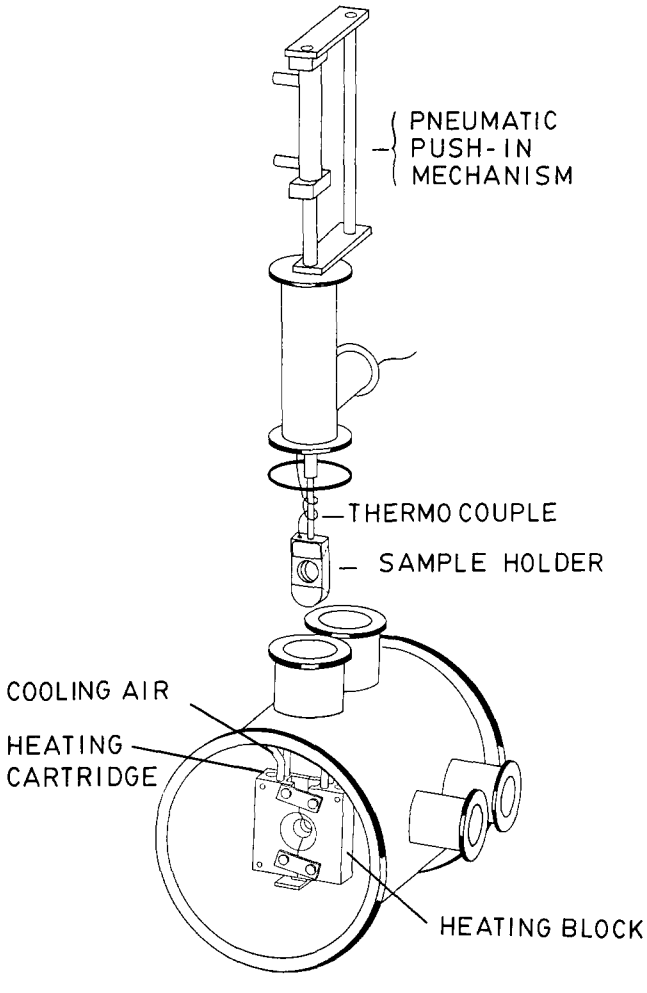

Figure 1 Furnace and device to shoot in the sample

EVALUATION OF THE SMALL-ANGLE X-RAY SCATTERING

Correction of the variation of the primary beam intensity

As described in the experimental section the intensity of the primary beam was measured in two different ways:

(1) by an ionization chamber which was passed by the beam before it reached the sample;

(2) by the detector behind the sample by using a semitransparent beam stop.

Figure 3 shows the effect of the correction of the scattering power Q with respect to variations of the intensity of the primary beam obtained by using the two different methods to monitor the primary beam. A crystallized PET sample was investigated at room temperature where one can be sure that no processes inducing changes of scattering occur. The scattering intensity of the sample was measured together with the power of the primary beam passing through the semitransparent beam stop. The intensity of the primary beam was reduced by an aluminium foil, 11.8 mm thick. Curve (a) represents the integral scattering intensity as a function of time without any correction. Curve (b) shows the integral scattering intensity divided by the power of the primary beam as measured by the ionization chamber. Curve (c) represents the integral scattering intensity divided by the integral intensity of the primary beam passing the semitransparent beam stop and measured by the Gabriel counter. It is obvious that the ionization chamber data do not correct the intensity fluctuations in the right way, whereas the data obtained by means of the semitransparent beam stop provide the appropriate correction.

Correction of the absorption

The monitoring of the primary beam intensity by means of a semitransparent beam stop is especially useful for correction of the background scattering. In order to do this correction it is necessary to know the absorption coefficient of the sample. This can be evaluated from the ratio of the primary beam intensities measured by the detector with and without the sample present in the beam. However, one has to take into account that only the third order of the Ge 111 reflection of the monochromator passes the aluminium in the beam stop while the first

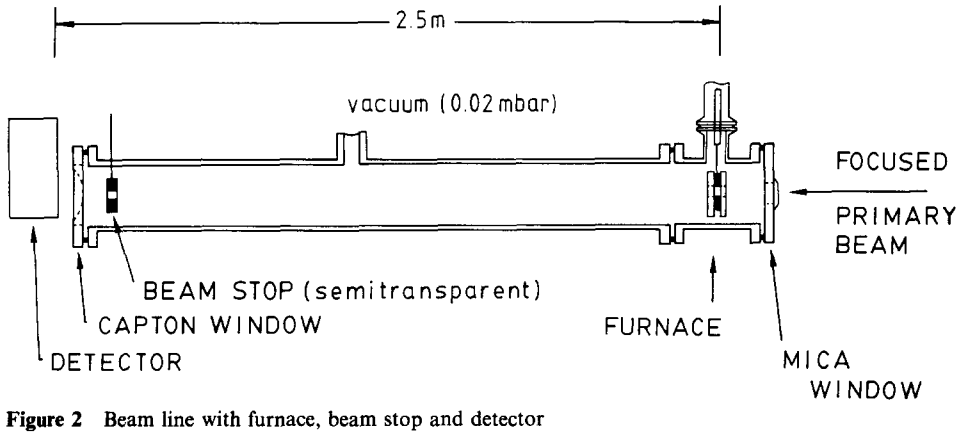

Figure 2 Beam line with furnace, beam stop and detector

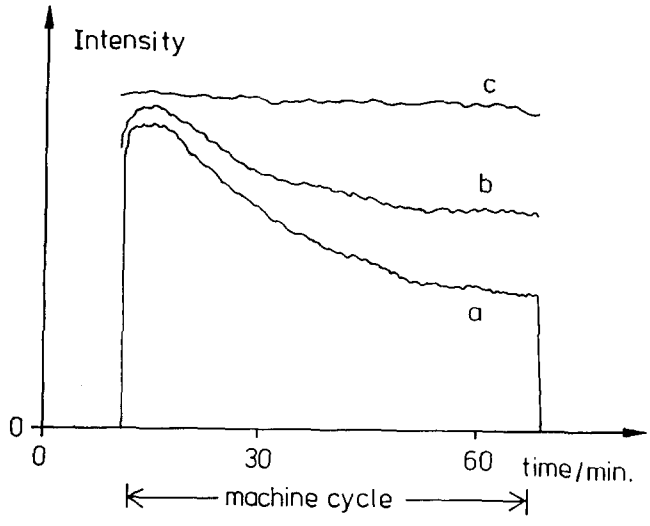

Figure 3 Example for the change of the integral scattering intensity of a crystalline PET sample during a machine cycle: (a) uncorrected data; (b) data corrected by ionization chamber; (c) data corrected by semitransparent beam stop

order is almost totally absorbed and the second order is absent. Therefore, we can only measure the absorption of the third-order reflection.

It is possible to calculate the absorption of the first-order reflection from that of the third order. If μ is the linear absorption coefficient per unit density, the decrease of the intensity due to absorption is generally given by $I = I_0 \exp(-\mu\rho d)$, I_0 being the intensity of the incident beam, ρ the density and d the thickness of the sample. If we denote the values corresponding to the wavelength of the third-order reflection by a prime and those corresponding to the wavelength of the first-order reflection without prime, we can write:

$$I/I_0 = \exp(-\mu\rho d) \tag{5}$$

and

$$I'/I_0' = \exp(-\mu'\rho d) \tag{6}$$

As

$$\exp(-\mu\rho d) = [\exp(-\mu'\rho d)]^{\mu/\mu'} \tag{7}$$

we find:

$$I/I_0 = (I'/I_0')^{\mu/\mu'} \tag{8}$$

The values of μ and μ' are listed in the literature[16] for different atoms and wavelengths. By using these data, the absorption coefficients μ and μ' of PET can be calculated as the mean values corresponding to the monomer unit. One obtains $\mu/\mu' = 16.36$. By inserting the calculated value of μ/μ' and the measured value of I'/I_0' into equation (8), the absorption I/I_0 is calculated.

Having typical counting rates of 10^3 per second and a sample thickness of 100 μm leading to an absorption factor I'/I_0' of 0.995, a data acquisition time of more than 5 min is necessary in order that the error in I/I_0 be less than $\pm 4\%$. For this reason the absorption of a given sample was measured only once at the beginning of an experiment and it was assumed that the absorption does not vary significantly with changes in the mean density during crystallization and melting.

Correction of the background scattering

In order to subtract from the total scattering the background scattering arising from different parts of the instrument, the background scattering that has been measured without a sample has to be corrected with respect to the absorption of the sample. If the primary beam—as measured using the semitransparent beam stop—was absorbed within the sample in the same manner as the background scattering then the normalization to the primary beam intensity would cancel not only differences in the intensity of the incoming beam but also any absorption effects. However, in our case, as only the intensity of the third order of the primary beam is measured, normalization with respect to the primary beam intensity only corrects the absorption corresponding to the third-order radiation. Therefore, the background correction is more complicated. An equation for correction is obtained by means of the following consideration.

The background scattering measured without the sample is designated by I_B. This function is normalized by dividing by the intensity of the primary beam I_0' (as measured by the detector after passing the aluminium foil in the beam stop). This yields the normalized background scattering:

$$\tilde{I}_B = I_B/I_0' \tag{9}$$

After the sample is inserted into the beam, owing to absorption in the sample, the background scattering is reduced to $I_B \exp(-\mu\rho d)$. In addition, the scattering is now normalized with respect to the primary beam intensity decreased by absorption, $I' = I_0' \exp(-\mu'\rho d)$. Thus, the intensity that has to be subtracted as a background from the normalized scattered intensity is given by:

$$\hat{I}_B = \frac{I_B \exp(\mu\rho d)}{I_0' \exp(\mu'\rho d)} \tag{10}$$

$\hat{I}_B$ can be calculated from the measured value I_B by means of the equation:

$$\hat{I}_B = \tilde{I}_B \frac{\exp(\mu\rho d)}{\exp(\mu'\rho d)} \tag{11}$$

By considering equations (6) and (7) one obtains:

$$\hat{I}_B = \tilde{I}_B \left(\frac{I'}{I_0'}\right)^{(\mu/\mu')-1} \tag{12}$$

Therefore, in order to perform the background correction, first the normalized background scattering without the sample, $\tilde{I}_B$, is measured. Afterwards, the relevant background scattering $\hat{I}_B$ is calculated by means of equation (12).

Figure 4 illustrates the effect of the background scattering correction procedure. Curve (a) represents the uncorrected scattering of a crystallized PET sample while curve (b) indicates the background scattering as measured with an empty sample holder. The background scattering increases sharply at small angles. Both curves are normalized with respect to the integral intensity of the primary beam and corrected with respect to absorption.

Determination of $\Delta\rho$ as a function of the temperature

Owing to the different thermal expansions of the crystalline and amorphous regions, $\Delta\rho = \rho_c - \rho_a$ changes with temperature. In order to determine the influence of this variation of $\Delta\rho$ on the scattering power Q during

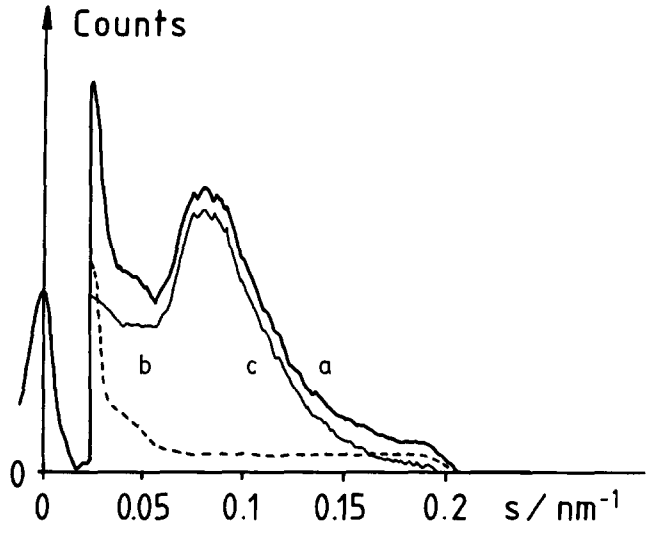

Figure 4 Small-angle X-ray scattering curve of a well crystallized sample (6 h at 230°C): (a) uncorrected scattering; (b) background scattering; (c) scattering corrected for background

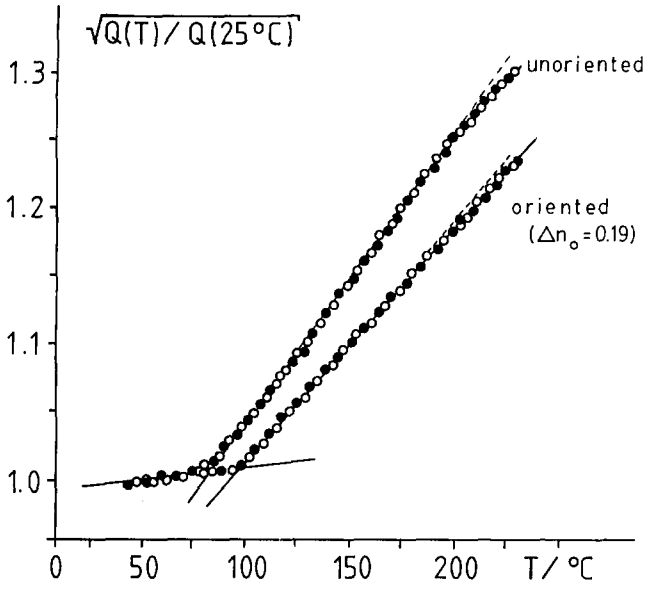

Figure 5 Square root of the scattering power Q of a well crystallized sample ($T_c = 235$°C) as a function of temperature: (●) during heating; (○) during cooling; (– – –) after correction of partial melting effects

heating and cooling, a sample was investigated which previously was crystallized at 235°C for 3 h and slowly cooled down to room temperature. After this pretreatment, upon heating no recrystallization occurs, provided the temperature remains lower than 235°C.

Figure 5 shows the change of the SAXS scattering power Q of this sample with temperature T during heating to 235°C and subsequent cooling with a constant rate of 3°C min^{-1}. The quantity $[Q(T)/Q(25°C)]^{1/2}$ is plotted against T, as suggested by equation (3), $Q(25°C)$ being the scattering power at $T_0 = 25$°C. The result is represented by two straight lines with different slopes intercepting at 72°C, the glass transition temperature of partially crystalline PET.

In addition, similar measurements have been performed on the highly oriented samples. The results are also represented in *Figure 5*. Again two straight lines are obtained. The slopes of these lines as well as the temperature at which they intercept are somewhat different from those obtained on the unoriented sample.

According to previous investigations[9], partial melting takes place not only in the melting range but also at temperatures below the temperature of crystallization, T_c. Of course, according to equation (1), the changes in the degree of crystallinity x_{cs} due to partial melting contribute to the measured variations of $Q(T)$. If one wants to obtain the variation of $Q(T)$ only caused by changes in $\Delta\rho$, the decrease in $Q(T)$ due to partial melting has to be eliminated.

In order to do this we have measured the partial melting in the following way. An initially amorphous PET sample was first crystallized at $T_c = 235$°C for 3 h and was then cooled slowly to room temperature. Separate parts of this sample were heated up quickly in a bath of silicone oil to different temperatures $T_a < T_c$. After 2 min of annealing they were quenched in iced water. The densities of all samples were measured at room temperature, and the overall crystallinities $x_c = V_s x_{cs}$ were calculated. *Figure 6* represents x_c as a function of the annealing temperature T_a. With increasing T_a the crystallinity of the quenched samples decreases slightly. Obviously partial melting has taken place at T_a and was frozen in by quenching. For the highly oriented samples the effect is smaller than for the isotropic ones.

By using these results the left-hand side of equation (4), $K_{T_0}(T)$, was calculated, which represents the change of $Q(T)$ caused only by changes of $\Delta\rho$. It was assumed that during partial melting, V_s does not change its value of 1. This is supported by microscopic observation. Therefore, in equation (4), $x_{cs} = x_c$ and $V_s = 1$. The result is represented in *Figure 5* by the broken lines. The deviations from the curve giving $[Q(T)/Q(25°C)]^{1/2}$ are small; however, they do improve the linearity of the curve.

Changes of the scattering power with temperature and time

An amorphous PET sample was crystallized at 120°C for 6 h. Then it was heated to 230°C and annealed at this temperature. *Figure 7a* shows the change in the SAXS curve as a function of time during the heating to 230°C and the following annealing. The corresponding course

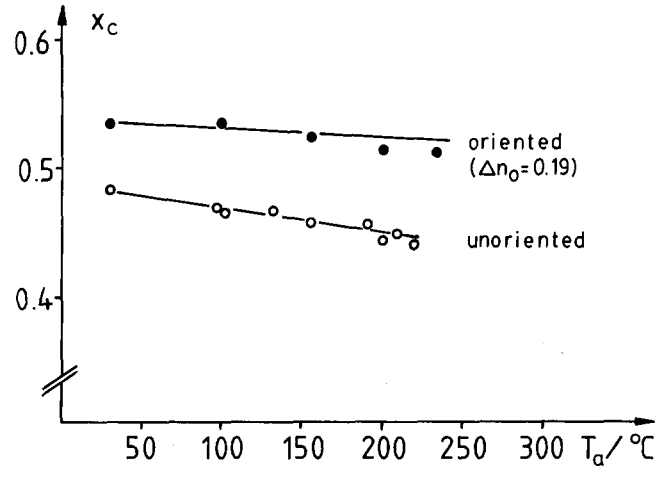

Figure 6 Degree of crystallinity x_c of a well crystallized sample (3 h at 235°C) as determined by density after annealing at T_a for 1 min and subsequent quenching in iced water as a function of T_a

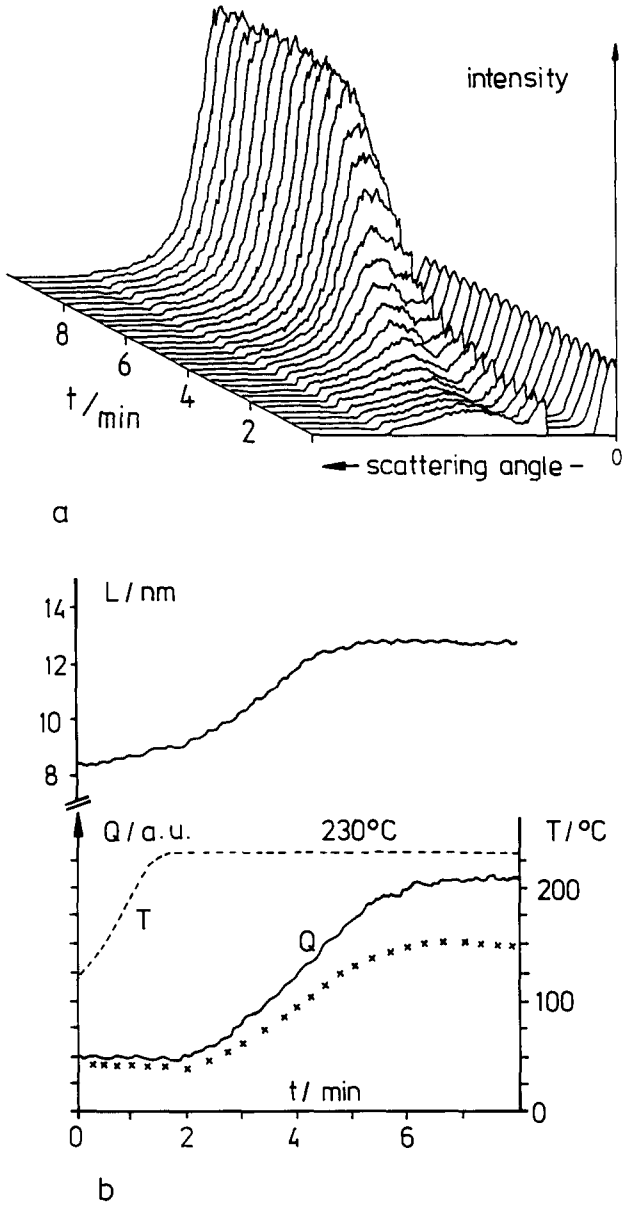

Figure 7 Change of small-angle X-ray scattering of a crystalline PET sample during heating to 230°C. The sample was previously crystallized at 120°C. (a) SAXS patterns. (b) Temperature T(– – –), scattering power Q (——) and scattering power Q corrected for thermal expansion (xxxx) as a function of time

of the temperature is shown in *Figure 7b*, together with the scattering power Q and the long period L. The latter is calculated by means of the Bragg equation from the angular position of the maximum of the scattering curve. It reflects the mean distance of two adjacent crystals. During the recrystallization process, the scattering intensity increases while the maximum of the intensity shifts gradually towards smaller angles.

Figure 8a shows the scattering curves obtained during stepwise heating and cooling of crystalline PET. The change of temperature T during the experiment is shown in *Figure 8b* where also the scattering power Q is plotted as a function of time. The sample was previously successively crystallized at 120, 230 and 235°C for 20 min at each temperature. During the first two cycles of the scattering experiment shown in the figure, the previous highest annealing temperature (235°C) is not exceeded. In this case, Q changes simultaneously and reversibly with temperature. These changes are mainly caused by changes in $\Delta\rho$, the density difference between the crystals and the amorphous regions. After heating up to 245°C, a slight decrease of Q is observed, which is caused by partial melting. During this partial melting the intensity of the original reflection decreases while an increase of the intensity at low angles can be seen in *Figure 8*.

This experiment was continued by performing two additional temperature cycles during which the sample was heated to 250°C, cooled down to 120°C and heated up to 250°C once more. The results are shown in *Figure 9*. During the first temperature increase, at the beginning an increase in the scattering power Q can be observed, which takes place simultaneously with the temperature increase and is due to different thermal expansions of the crystalline and amorphous regions. However, before the temperature of 250°C is reached, melting takes place, reducing Q rapidly to a small value. After this, recrystallization starts, which is reflected in the slow increase of Q following the melting. This increase of Q is caused mainly by an intensity increase of a peak at very low angles.

The subsequent cooling of the sample to 120°C is accompanied by a rapid increase of Q, while the peak at small angle decreases. At the low temperature, a reflection

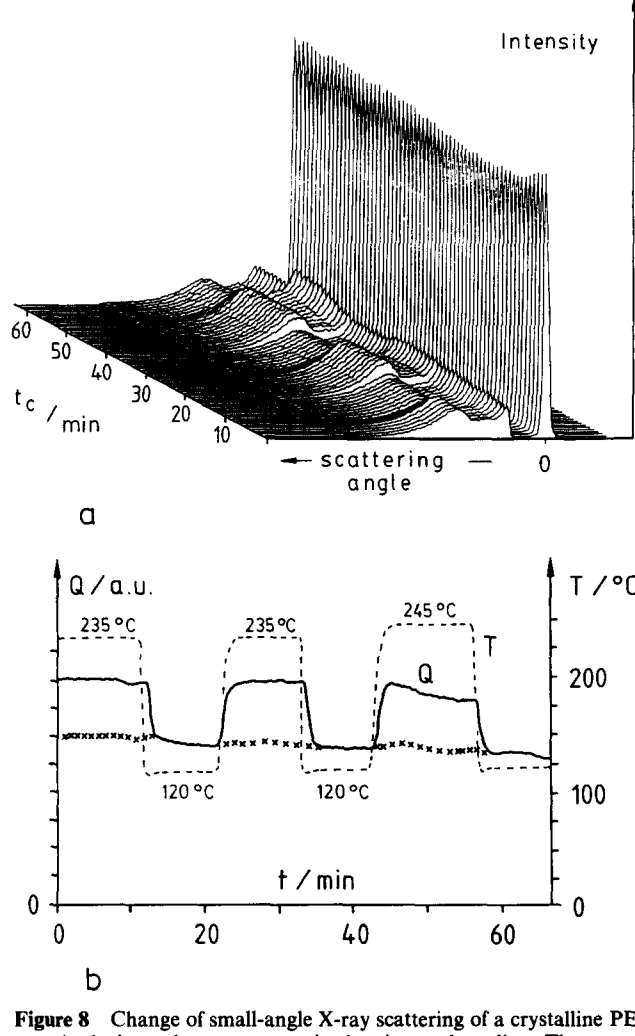

Figure 8 Change of small-angle X-ray scattering of a crystalline PET sample during subsequent stepwise heating and cooling. The sample was previously crystallized at 120, 230 and 235°C. (a) SAXS patterns. (b) Temperature T (– – –), scattering power Q (——) and scattering power Q corrected for thermal expansion (xxxx) as a function of time

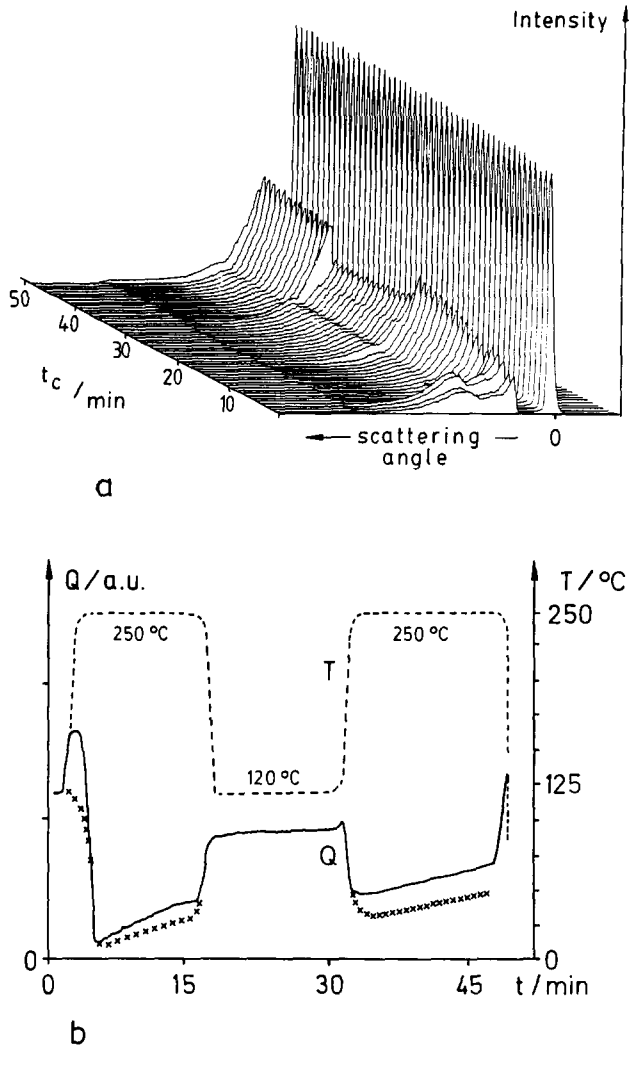

Figure 9 Change of small-angle X-ray scattering of a crystalline PET sample during subsequent heating and cooling. The sample was previously crystallized at 120, 230, 235 and 245°C. (a) SAXS patterns. (b) Temperatures T (---), scattering power Q (——) and scattering power Q corrected for thermal expansion (xxxx) as a function of time

appears almost at the same position at which the reflection had been before the melting at 250°C took place.

After heating up again to 250°C, Q is reduced to the value that was reached just before cooling was performed. At the same time the peak at large scattering angle vanishes. After this, recrystallization proceeds and Q increases. The peak at small scattering angle grows again.

If, from the changes of Q, one wants to determine the melting and recrystallization quantitatively, one has to subtract from the change of Q the part of the change caused by the different thermal expansions of the crystalline and amorphous regions. After this correction, according to equation (1) the variation of Q only reflects changes in the degree of crystallinity x_{cs} and the volume fraction of spherulitically crystallized material V_s. The correction can be made with the aid of the data of *Figure 5* using equation (3). This has been performed with the values of Q in *Figure 8* taking 120°C as reference temperature T_0. The results are represented in *Figure 8b* by the curve marked by crosses. During the first three temperature cycles the corrected values of Q remain constant. This proves that the changes of the uncorrected values of Q are caused by thermal expansion effects. During the last cycle in *Figure 8*, the corrected values of Q indicate that some melting occurs. A similar correction was performed with the Q values in *Figure 7*.

The Q values in *Figure 9* were corrected with respect to thermal expansion effects, too. In order to be able to do this, the curve shown in *Figure 5* had to be extrapolated to higher temperatures. The corrected values of Q are represented by crosses in *Figure 9b*. As one can see, after the correction, the increase of Q observed at the beginning of the first heating to 250°C disappears. Obviously, this increase is solely an effect of thermal expansion.

Determination of changes in V_s and x_{cs}

After the Q values of a recrystallization experiment have been corrected for the thermal expansion effect, the residual changes in Q are either due to changes in V_s or to changes in x_{cs} in equation (1). In the first case large parts of spherulites melt and are formed again. In the second case the spherulitic fine structure is changed, for example lamellae may become thicker or single lamellae may melt, while V_s is constant (equal to 1).

By comparing the change of Q with the change of the overall crystallinity x_c as measured by WAXS, it can be determined whether the change of Q is caused by a variation of V_s or of x_{cs}. As can be seen from equations (1) and (2), if only V_s changes, the scattering power Q is directly proportional to V_s and therefore proportional to the overall degree of crystallinity x_c. In contrast, if x_{cs} varies while $V_s=1$ then Q is proportional to $x_{cs}(1-x_{cs})$ and therefore proportional to $x(1-x)$.

In more detail, if we designate the values at the end of the recrystallization process by the index e and the values changing during recrystallization without index e, we can write according to equation (1):

$$\frac{Q}{Q_e}=\frac{V_s x_{cs}(1-x_{cs})}{V_{se}x_{cse}(1-x_{cse})} \tag{13}$$

If x_{cs} is constant we have, according to equation (1), $V_s/V_{se}=x_c/x_{ce}$ and we obtain:

$$x_c=(x_{ce}/Q_e)Q \tag{14}$$

By means of this equation x_c can be calculated from the measured values of Q if x_{ce} is known (for example from WAXS). In contrast, if $V_s=1$, we obtain $x_c=x_{cs}$ and equation (13) goes over into:

$$\frac{Q}{Q_e}=\frac{x_c(1-x_c)}{x_{ce}(1-x_{ce})} \tag{15}$$

This is a quadratic equation for x_c, again allowing x_c to be calculated from the measured values of Q.

In *Figure 10*, for the recrystallization experiment represented in *Figure 7*, the overall degree of crystallinity x_c as measured by WAXS is plotted as a function of time (full circles). In addition, x_c was calculated from Q by using equation (14) and (15) giving the broken curve and the full curve, respectively. The full curve represents the values obtained under the assumption $V_s=1$; the broken curve represents the values obtained assuming that x_{cs} is constant. The value of x_{ce} in equation (14) and (15) was chosen in agreement with the WAXS value at the end of crystallization. Therefore, at large crystallization times, all curves fall together. As can be seen, the curve calculated under the assumption of a constant value V_s

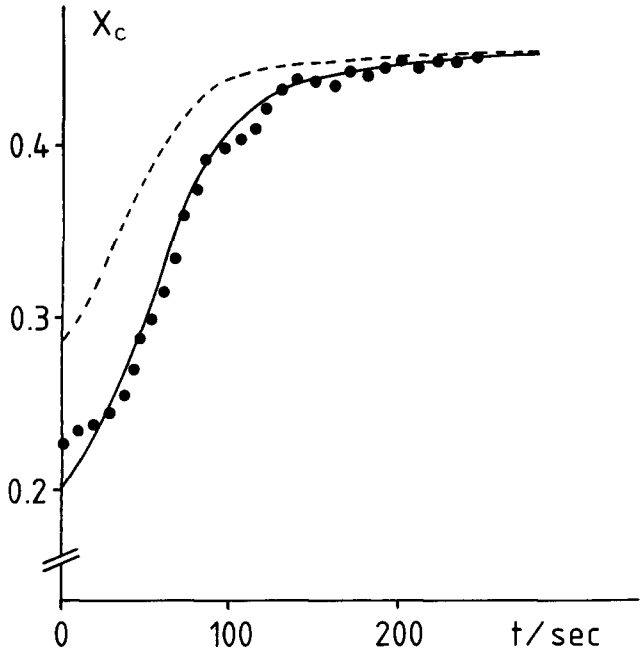

Figure 10 Degree of crystallinity x_c during recrystallization of an unoriented sample at 230°C (T_c=120°C) as a function of time (see *Figure 7*): (●) from wide-angle X-ray scattering; (---) from SAXS power Q assuming V_s is increasing and x_{cs} is constant; (——) from SAXS power Q assuming x_{cs} is increasing and V_s=1

agrees fairly well with the full circles. From this it is deduced that, during recrystallization, changes of the fine structure within the spherulites take place. The formation of new regions of staggered lamellae, which would increase V_s and lead to an increase of Q shown by the broken curve, can be excluded.

DISCUSSION

Thermal expansion

The plot in *Figure 5* leads to a linear dependence, according to equations (3) and (4) respectively. Two distinct temperature regions showing different slopes can be identified. The lower one belongs to the region below the glass transition temperature T_g of the amorphous regions. Below T_g the thermal expansion of the crystalline as well as of the amorphous regions is primarily determined by oscillations of single atoms. Because of the similar expansion mechanism, the value of $\alpha_a-\alpha_c$ and therefore also the slope of the $\sqrt{Q}$ *versus* T curve is small. Above T_g, the mechanism of thermal expansion of the crystals remains the same as below T_g while in the amorphous regions the atoms may jump to new locations in addition to their oscillatory motion. An increasing number of vacancies is created on raising the temperature. This leads to a sharp increase of α_a, resulting in a change of the slopes of the curves in *Figure 5*.

The influence of partial melting on the curves of *Figure 5* is rather small compared to the changes due to thermal effects. According to equation (1) this influence is reduced particularly by the fact that the degree of crystallinity is close to 0.5.

The values of T_g and $\alpha_a-\alpha_c$ obtained from the curves in *Figure 5* are summarized in *Table 1*.

For $T>T_g$ the $\alpha_a-\alpha_c$ values are in good agreement with those found by Fischer and Fakirov[17], who used the relative maximum intensities of the SAXS instead of the Q values.

It is remarkable that below T_g a slope of the $\sqrt{Q}$ *versus* T curves is observed which is different from zero. Choy *et al.*[18] have measured the thermal expansion coefficients of oriented and unoriented PET fibres below the glass transition temperature, between −153 and +25°C. To obtain the thermal expansivity at 65°C just below T_g, we had to extrapolate their data to this temperature. By linear extrapolation we estimate $\alpha_a=8.7\times10^{-5}$ °C^{-1} for the amorphous unoriented material. Linear thermal expansivity coefficients of the PET crystal were obtained from lattice parameter measurements by means of wide-angle X-ray scattering[19]. The value $\alpha_{1c}=2.2\times10^{-5}$ °C^{-1} was obtained for expansion parallel to the chain direction and the value $\alpha_{2c}=14.9\times10^{-5}$ °C^{-1} was found for expansion perpendicular to the chain direction. These values can be assumed to be independent of temperature. The mean thermal volume expansion coefficient of the crystals is thus the mean value over all three directions:

$$\alpha_c=\alpha_{1c}+2\alpha_{2c}=2.8\times10^{-4}\ °C^{-1}$$

From this it follows that just below T_g the difference of the linear thermal volume expansion coefficients of the crystalline and non-crystalline regions should be about 1.9×10^{-4} °C^{-1}, which is in good agreement with our results.

With the oriented samples, one obtains SAXS diagrams forming layer lines on the meridian. With the geometry realized in our measurements we obtain the intensity only along the meridian. The integral intensity in this direction corresponds to the total scattering power if we assume that the azimuthal profile of the reflection does not change with temperature. On the other hand, it is known that the thermal expansion of oriented polymers is strongly anisotropic. This may influence the shape of the SAXS pattern as a function of temperature. If we neglect this problem, we have to conclude from the results presented in *Figure 5* that, for the highly oriented material, T_g is higher and $\alpha_a-\alpha_c$ is lower than for the unoriented one. The increase of T_g due to orientation can be explained by a decrease of the free volume when the chains in the non-crystalline regions are forced to become parallel. The decrease of $\alpha_a-\alpha_c$ can be explained in a similar way. Above T_g, α_a is larger than α_c, leading to the observed positive slope of the curves in *Figure 5*. When the amorphous regions are oriented, α_a decreases because the local rearrangements of parts of the chains become more and more hindered. In an extremely highly oriented material α_a will be almost identical to α_c and T_g becomes meaningless. This suggests a method for investigation of the orientation of the chains within the non-crystalline regions of partially crystallized drawn material.

Table 1 Glass transition temperature T_g and difference of thermal expansivity coefficients between the crystalline and non-crystalline regions ($\alpha_a-\alpha_c$) for unoriented and oriented PET

		$\alpha_a-\alpha_c$ (°C)	
Sample	T_g (°C)	$T>T_g$	$T<T_g$
Unoriented	76.2	2.0×10^{-3}	1.5×10^{-4}
Oriented	93.1	1.7×10^{-3}	1.6×10^{-4}

Partial melting and recrystallization

The work described in the present paper provides a method for quantitative evaluation of the time dependence of partial melting and recrystallization. Such investigations have already been performed earlier with quenched samples[9]. By using the method presented here, these measurements can also be performed with materials in which it is not possible to freeze in the partially molten states.

Partial melting occurs quickly, almost within the time of heating. Only if the temperature is just below the former crystallization temperature does partial melting seem to be a relatively slow process, as can be seen in *Figure 8*. Here, the last temperature increase is followed by a slow decrease of Q, which is due to partial melting.

Recrystallization usually takes place slower than partial melting. It can be followed easily by the method described here. Results concerning the influence of temperature, molecular weight and orientation on the course of partial melting and recrystallization are presented elsewhere[20].

A comparison of the variation of Q with that of the overall crystallinity $x_c = V_s x_{cs}$ as measured by wide-angle X-ray scattering or density made it possible to determine whether V_s or x_{cs} in equation (1) is changing during partial melting and recrystallization. Thus, one can decide whether partial melting and recrystallization takes place within the lamellar structures that build up the spherulites or whether larger parts of spherulites melt and recrystallize. The results presented in *Figure 10* suggest that the first model is true. This is in agreement with investigations by optical microscopy, which have shown that the spherulitic structure does not change during recrystallization.

In contrast, in the case of isothermal crystallization starting from the amorphous state, simultaneous measurements[21] of small- and wide-angle X-ray scattering show that Q is proportional to the overall crystallinity x_c. This implies that the isothermal crystallization from the amorphous state takes place by the growth of spherulites while the internal lamellar structure of the spherulites does not change significantly.

During the recrystallization shown in *Figure 7* the scattering power and the long period gradually increase. At the present stage of the investigations it is not possible to decide whether this is due to a continuous increase of the thickness of the lamellae or to a melting of small lamellae accompanied by growth of thicker ones. A more detailed answer to this question is given in another paper, where the influence of molecular weight, orientation and temperature on the kinetics of recrystallization is discussed[20].

ACKNOWLEDGEMENT

This work has been funded by the German Federal Ministry for Research and Technology (BMFT) under contract number 05305 HXB.

REFERENCES

1 Elsner, G., Koch, M. H. J., Bordas, J. and Zachmann, H. G. *Macromol. Chem.* 1981, **182**, 1263
2 Elsner, G., Zachmann, H. G. and Milch, J. R. *Makromol. Chem.* 1981, **182**, 657
3 Grubb, D. T., Liu, J. J. H., Caffey, M. and Bilderback, D. H. *J. Polym. Sci., Polym. Phys. Edn.* 1984, **22**, 367
4 Russel, T. P., Hadziioannou, G. and Warburton, W. K. *Macromolecules* 1985, **18**, 78
5 Barham, P. J. *Europhys. Conf. Abstr. (D)* 1988, **12**, 48
6 Elsner, G., Riekel, C. and Zachmann, H. G. *Adv. Polym. Sci.* 1985, **67**, 1
7 Hendrix, J. *Adv. Polym. Sci.* 1985, **67**, 59
8 Fischer, E. W., Kloos, F. and Lieser, G. *Polym. Lett.* 1969, **7**, 845
9 Zachmann, H. G. and Stuart, H. A. *Makromol. Chem.* 1960, **41**, 148
10 Zachmann, H. G. and Schmidt, G. F. *Makromol. Chem.* 1962, **52**, 23
11 Günther, B. and Zachmann, H. G. *Polymer* 1983, **24**, 1008
12 Moore, L. D. *Polym. Prepr.* 1960, **1**, 234
13 Gehrke, R. and Zachmann, H. G. *Makromol. Chem.* 1981, **182**, 627
14 Hendrix, J., Koch, M. H. J. and Bordas, J. *J. Appl. Crystallogr.* 1979, **12**, 467
15 Gabriel, A. *Rev. Sci. Instrum.* 1977, **48**, 1303
16 'International Tables for X-Ray Crystallography', Vol. III, Kynoch Press, Birmingham, 1968
17 Fischer, E. W. and Fakirov, S. *J. Mater. Sci.* 1976, **11**, 1041
18 Choy, C. L., Ito, M. and Porter, R. S. *J. Polym. Sci., Polym. Phys. Edn.* 1983, **21**, 1427
19 Wakelin, J. H., Sutherland, A. and Beck, L. R. *J. Polym. Sci.* 1960, **42**, 278
20 Gehrke, R. and Zachmann, H. G. to be published
21 Prieske, W., Zachmann, H. G. and Koch, M. H. J. to be published